Journal of the American Mosquito Control Association, 39(1):18–30, 2023

USE OF A MINIATURE OPTICAL ENGINE FOR AGE CLASSIFYING WILD-CAUGHT *COQUILLETTIDIA PERTURBANS* IN THE SHORTWAVE INFRARED REGION

CHRISTOPHER L. SWAB,[1] CURTIS R. BEST,[2] FRANK H. CORNINE III,[2] DAVID R. SEGAL[2] AND SAM R. TELFORD III[1]

ABSTRACT. Near-infrared spectroscopy (NIRS), coupled with modeling and chemometrics, has been used to age grade anopheline and aedine mosquitoes; however, NIRS has not been widely used in field studies to assign mosquitoes to age classes. One reason is the relative cost of NIRS spectrometers. We developed a spectrometer system incorporating a miniature optical engine generating spectra in the shortwave infrared region, calibrated it using laboratory-reared *Aedes aegypti*, and evaluated its utility to age grade wild-caught cattail mosquitoes, *Coquillettidia perturbans*. As a refinement of the method, we compared a scoring system based on spectral data point outliers with the typical chemometrics that have been used with NIRS. This inexpensive system (<$3,600) could reliably discriminate between age cohorts of mosquitoes and has the potential for more detailed age grading. Laboratory-reared *Ae. aegypti* demonstrated a decline in the fraction of spectral outliers with age, and field-collected *Cq. perturbans* similarly demonstrated such a decline (greater in newly emerged mosquitoes) with date of collection, consistent with their univoltine demography in Massachusetts. We conclude that an economical NIRS system may be able to provide a quantitative dichotomous (young versus old) assessment of field-collected mosquito samples, and thereby may be used to complement abundance-based analyses of the efficacy of adulticiding applications.

KEY WORDS Cattail mosquito, low-cost compact spectrometer, shortwave infrared, spectral outliers, spectroscopy

INTRODUCTION

The use of aerial or ground-based spraying of insecticides is intended to reduce the abundance of nuisance mosquitoes, and also lower the risk of humans acquiring mosquito-borne infections after surveillance indicates a risk threshold. Adulticiding intended as nuisance abatement may have the added benefit of preventing arboviral infections when the most prevalent human-biting species also serve as the main vectors in a localized area. Evaluating the effects of adulticiding can be difficult; although abundance indices derived from mosquito trapping are used, they are prone to confounding due to limitations of adequate sampling, and by the continued emergence of new mosquitoes from breeding sites. For public health purposes, the objective of adulticiding is to reduce the older cohorts of mosquitoes in which the infectious agent has survived the extrinsic incubation period rendering the mosquitoes infective. Age grading and in particular parous rates were used effectively to confirm the effects of antimalarial interventions (Garrett-Jones and Grab 1964). Classical methods of age grading and determinations of parous rates, however, are time consuming, requiring the dissection of mosquito ovaries and microscopic examination, but remain the gold standard. Such methods are not likely to be used routinely for most public health interventions due to the time and expertise required.

Near-infrared spectroscopy (NIRS) has been used to characterize wild-caught malaria-vector mosquitoes, including age grading of nulliparous and parous cohorts (Sikulu et al. 2010, Joy et al. 2022), estimating age distribution based on exposure to pyrethroids (Sikulu et al. 2014), defining binary age classes with partial success (Krajacich et al. 2017), and assessing parity status (Milali et al. 2020). To date, mosquitoes have been investigated by this method using expensive, laboratory-grade spectrometers and reflectance standards. Spectra from these studies typically fall within the region of 900–2,500 nm, and chemometrics for spectral evaluation have varied from regression or partial least squares (PLS-1) modeling to autoencoders coupled with artificial neural networks. Methods involving NIRS that have been developed have not been widely adopted by mosquito ecologists. There are at least 2 reasons for this: expense of equipment and relatively poor performance in the field. Based on e-commerce company listings, a current estimate for a preowned benchtop spectrometer similar to those used in prior studies is US$10,000 to $15,000 or higher depending on the model. Poor performance in the field may be due to the fact that larval diets in nature are very different than what is used in the lab, and the gut microbiome may affect the expression of chemical signatures (Liebman et al. 2015, Martinson and Strand 2021).

There have been new developments in NIRS technology, and we sought to leverage these. We sought to construct, validate, and use an economical

[1] Department of Infectious Disease and Global Health, Cummings School of Veterinary Medicine, Tufts University, 200 Westboro Road, North Grafton, MA 01536.

[2] Central Massachusetts Mosquito Control Project, 111 Otis Street, Northborough, MA 01532.

system for a very defined application, to distinguish between "new" and "old" mosquitoes, instead of trying to be able to assign them to a more finely grained estimate of specific days of life. In particular, we sought to provide the basis to evaluate adulticiding activities directed against the main vector for eastern equine encephalitis virus (EEEV) in Massachusetts, the cattail mosquito *Coquillettidia perturbans* (Walker). Documenting efficacy of these activities has relied mainly on pre- and postspray abundance estimates, which can vary for diverse logistical reasons. The capacity to determine the proportion of newly emerged to older *Cq. perturbans* has the potential to complement abundance indices and help demonstrate that adulticiding reduces EEEV transmission risk: evidence of a successful intervention would be a demonstration that the mosquito populations that remain after insecticidal application are newly eclosed and thus have not acquired virus. Accordingly, we built an economical system, validated it against laboratory-reared *Aedes aegypti* (L.) to demonstrate equivalency with previously published NIRS methods, compared a simple spectral outlier analysis with the NIRS standard of modeling and chemometrics, and applied our system to collections of the main EEEV bridge vector in Massachusetts.

MATERIALS AND METHODS

Construction of the NIRS system

Our scanning setup consisted of a Texas Instruments DLP® NIRscan™ Nano spectrometer (DLPNIRNANOEVM; Texas Instruments Inc., Dallas, TX), a stabilized tungsten light source (SLS201L; Thorlabs, Newton, NJ), and a 200-μm fiber-optic reflectance probe with a linear leg (RP25; Thorlabs). The spectrometer differs from conventional instruments in that it is a compact evaluation module that utilizes a digital micromirror device to focus wavelengths of light to the detector. The spectrometer generates spectra in the shortwave infrared (SWIR) region (900–1,700 nm), a range that contains intervals determined to be optimal for age grading of *Anopheles* and *Aedes* mosquitoes (Lambert et al. 2018). Its digital resolution is 3.5 nm, resulting in 228 data points per spectrum provided as absorbance units (AU). The factory-fitted illumination module on the spectrometer was removed and the probe connected via a fiber input chassis (TI PN2513928; Milltech Mfg. Inc., Garland, TX) fitted with 2 collimating aspheric lenses (354171-C; Thorlabs) for light wave alignment. We used a reflectance standard consisting of a 15-cm-diam cork disk wrapped in matte polytetrafluoroethylene (PTFE) thread-seal tape tape (Lowe's Companies Inc., Mooresville, NC), which when layered to sufficient thickness has a reflection coefficient comparable to laboratory-grade reflectors (Janecek 2012).

As an initial test of the accuracy of our scanning setup, we scanned an aspirin pill for comparison to manufacturer testing data (Texas Instruments Inc. 2015). Test scans of uncoated aspirin pills (CVS Pharmacy Inc., Woonsocket, RI), using a variety of probe angles and heights, showed that spectral noise was considerably reduced the closer the probe was to the pill surface, with the cleanest spectra obtained with the probe at an angle of 90° and in contact with the pill surface. Standard normal variate (SNV) preprocessing of aspirin spectra yielded spectral peaks and valleys at wavelengths consistent with those in the spectrometer technical documentation (Fig. 1), and as such SNV was chosen as the preprocessing technique for this work. To position the probe as consistently close as possible to, but not touching the surface of each mosquito, a microscope stand with a precision elevator platform for fine height adjustment (Z008; Shenzhen Supereyes Co., Guangdong, China) was used to hand-focus the probe head to within approximately 1 mm of the cuticle for each scan. The spectrometer and stand were enclosed in rudimentary cabinetry manufactured in-house from plywood and locally purchased hinges and fasteners. The cabinetry was constructed to eliminate any potential impact from ambient light during scanning and consisted of 2 small boxes of 0.005 m^3 for the spectrometer and 0.02 m^3 for the stand. The complete setup is shown in Fig. 2.

Calibration using laboratory-reared Ae. aegypti

Aedes aegypti (Black eye Liverpool, NR 48921; BEI Resources, NIAID, NIH) larvae were reared at 26°C using a diet of commercial guinea pig chow. Pupae were separated into containers on a daily basis and provided with sugar and water ad libitum. A large cohort was sampled every 3 days for 3 wk and was frozen at each sampling point at –20°C. Mosquitoes were thawed and positioned with no further specimen preparation, and the lateral thorax of female mosquitoes was scanned using the compact spectrometer limited to the SWIR region of 900–1,700 nm.

Comparison of modeling analysis of spectra with simplified spectral outlier analysis

As a calibration check, we conducted modeling on the spectra from the lab-reared *Ae. aegypti* from our study and Sikulu-Lord et al. (2016) using GRAMS IQ Spectroscopy Software (Thermo Fisher Scientific, Waltham, MA). Models were trained on each sample with a calibration type of partial least squares with leave one out as cross validation (PLS-1), following the modeling setup used in prior studies (Johnson and Naiker 2020). To ensure a commensurate comparison between scanning systems, only wavelengths corresponding to our spectrometer's resolution were used and data were converted from reflectance to absorbance ($A = \log 1/R$). The minimum cohort age for

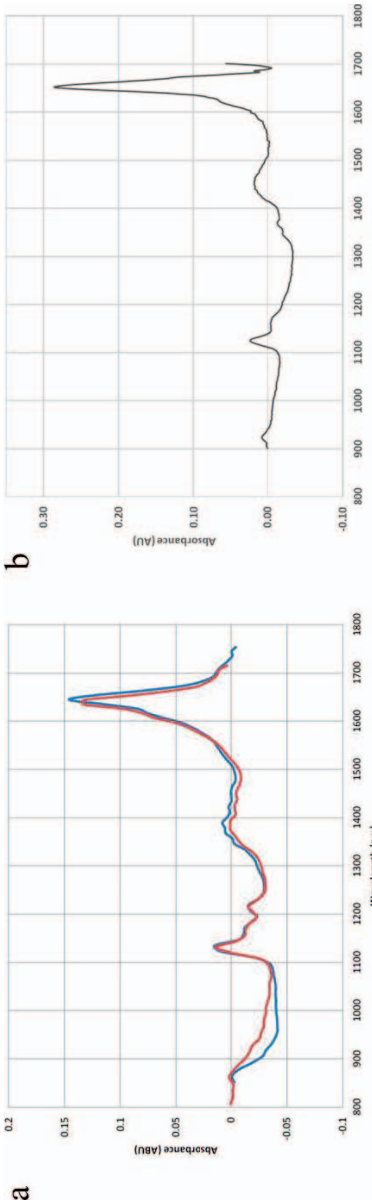

Fig. 1. The NIRscan™ Nano spectrometer, aspirin test scanning results for verification of the setup used in this study. (a) Texas Instruments technical documentation, spectrometer with factory-fitted illumination module, normalized data (Texas Instruments Inc. 2015). (b) This study; uncoated aspirin pill, spectrometer with reflectance probe configuration and probe at 90° angle, average of 100 scans, standard normal variate (SNV) spectra preprocessing.

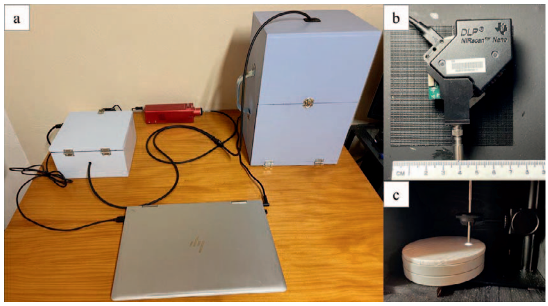

Fig. 2. Spectroscopy setup. (a) Full setup showing cabinetry and fixed light source. (b) Spectrometer with chassis and probe leg attached. (c) Microscope stand with probe and reflectance standard disk.

both studies was 1 day, whereas the maximum cohort ages were 30 days for our study and 20 days for Sikulu-Lord et al. (2016). Models were trained on young (≤7 days) versus old (>7 days) groups, with weighted average age per group selected as values. Spectral preprocessing for both models consisted of mean centering with Savitzky–Golay smoothing of between 9 and 13 points, parameters that generated the highest actual to predicted age linear correlation in training sets.

Collection and scanning of Cq. perturbans

Cattail mosquitoes were collected during the 2021 and 2022 seasons at 5 trap sites in central Massachusetts, USA. All sites were located within 15 km of Cedar Swamp, an 1,100-ha wetland east of the town of Westborough where these mosquitoes have historically been abundant (Commonwealth of Massachusetts, Department of Public Health, State Laboratory Institute 2022), in a variety of environments, including adjacent to wetlands, in residential areas, and near roadways (Fig. 3). A Centers for Disease Control and Prevention miniature light trap with CO_2 as an attractant was used for all trapping. To ascertain the impact of different larval habitats on our analysis, trap sites A and B were used for 2021 seasonal trend analysis whereas trap site D was selected for 2022 seasonal trend analysis.

Mosquitoes were frozen at –40°C immediately after collection and then kept frozen at –10°C for between 1 to 3 days prior to scanning. Storage time fell well within the 2-month preservation period deemed acceptable by Dowell et al. (2011), while freezing was chosen as this was the preservation method used in recent studies by Sikulu-Lord et al. (2016) and Ong et al. (2020). To increase spectral precision the spectrometer was set to automatically take 60 scans and generate an average spectrum each time the scan button was activated. Mosquitoes were oriented with the probe focused on the lateral thorax region, with care taken to remove wings and legs from the scanning area and orient all mosquitoes in the same direction. Mosquitoes were typically

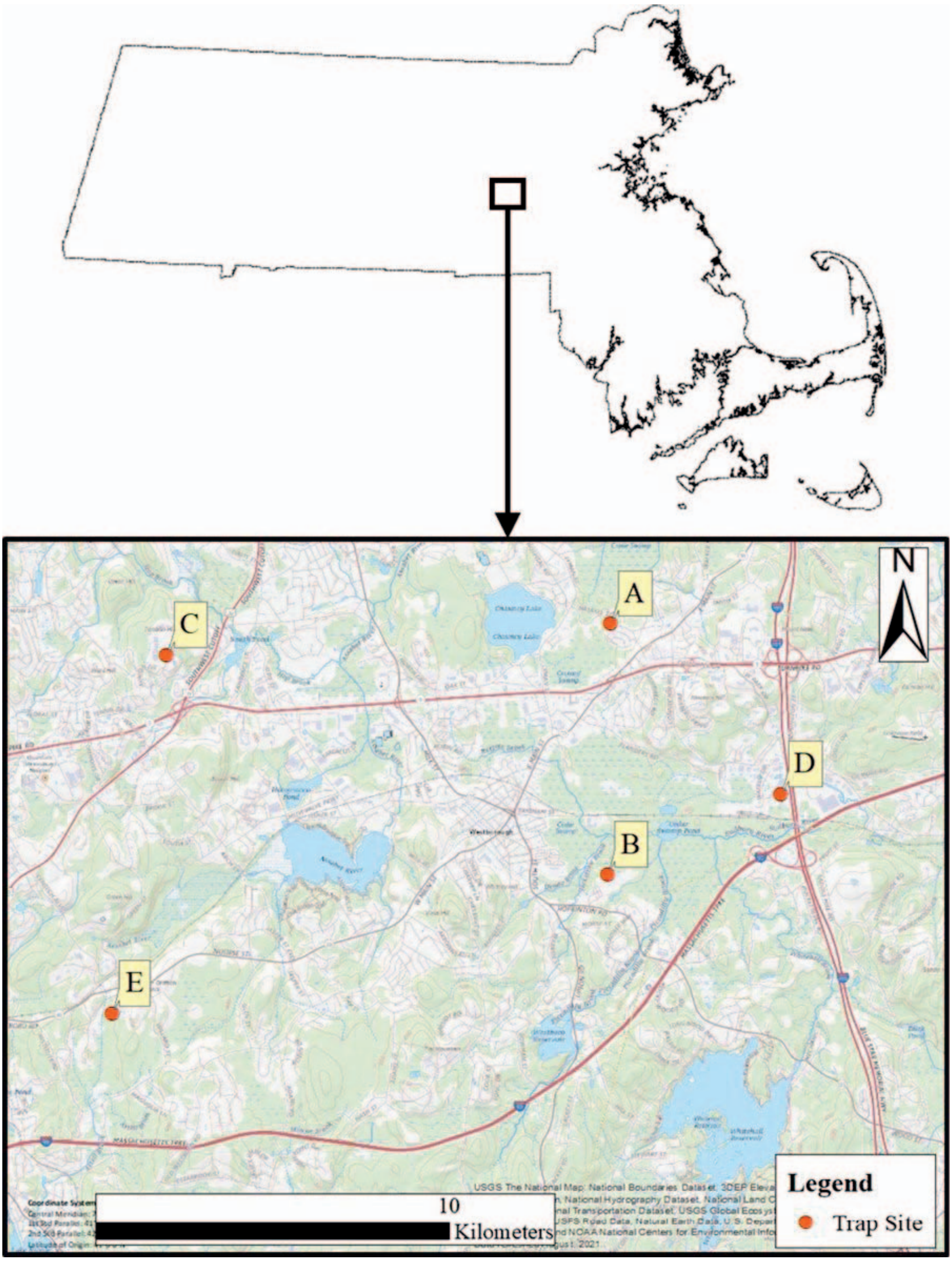

Fig. 3. Trap sites in 2021 and 2022; trap type = Centers for Disease Control and Prevention (CDC) miniature light trap with CO_2 as an attractant. See Table 3 for collection dates, abundance, and scanning details.

scanned in batches of 20, and each batch was scanned twice consecutively, resulting in 2 duplicate scans per mosquito. Duplicate scanning was done to increase spectral precision, which is partly dependent on scanning operator skill and consistency (Williams 2013). A background check was run once per batch, e.g., 40 scans to verify that lamp intensity and PTFE background absorption readings remained stable.

Mosquitoes with and without parasitic water mites were scanned separately to determine if mites had an impact on outlier fraction. For the 2021 season, mite-infested mosquitoes from all collections were

Table 1. Cost breakdown in US dollars (USD) of the equipment used in this study.

Component or equipment	Manufacturer	USD
Spectrometer		
DLP® NIRscan Nano Evaluation Module	Texas Instruments Inc. (Dallas, TX)	$999.01
Subtotal		$999.01
Fiber input module		
Chassis assembly, fiber input module	MillTech Manufacturing, Inc. (Garland, TX)	$335.00
Nut plate, Subminiature version A connector	MillTech Manufacturing, Inc. (Garland, TX)	$330.00
Lenses: 354171 with plano surface	Thorlabs, Inc. (Newton, NJ)	$115.26
Subminiature version A fiber-optic bulkhead adapter	Thorlabs, Inc. (Newton, NJ)	$8.55
Subtotal		$788.81
Fiber optic scanning components		
Stabilized fiber-coupled light source with universal power adapter, 360–2,600 nm, 1/4″-20 taps	Thorlabs, Inc. (Newton, NJ)	$1,092.94
Reflection probe with linear leg, Ø200 µm, 400–2,400 nm, SMA to Ø1/4″ probe, 2 m long	Thorlabs, Inc. (Newton, NJ)	$604.91
Subtotal		$1,697.85
Probe stand and reflectance standard		
Z008 Adjustable precision microscope stand	Shenzhen Supereyes Co., Ltd. (Guangdong, China)	$45.00
15-cm-diam cork disk	Amazon.com, Inc. (Seattle, WA)	$1.62
Teflon tape (matte)	Lowe's Companies Inc. (Mooresville, NC)	$2.58
Subtotal		$49.20
Cabinetry for the spectrometer, probe stand/reflectance standard		
Plywood, hinges, fasteners	Manufactured in-house	$30.00
Subtotal		$30.00
Total		$3,564.87

scanned as a single batch for comparison to results from mosquitoes without mites. As a refinement in 2022, mite-infested mosquitoes were scanned for trap sites A, B, C, D, and E by various collection dates for comparison to mosquitoes without mites from the same collections.

Modeling, outlier analysis, and age classification of Cq. perturbans

We conducted modeling on the 2021 *Cq. perturbans* collections with the intent of showing similarities or differences between collections of different dates. Discriminatory (dichotomous) models were trained on cohorts of wild-caught *Cq. perturbans* by collection date. The software and procedure followed the method described above for the modeling of laboratory-reared *Ae. aegypti*.

We conducted a simplified analysis of outliers as a fraction of total spectral data points for *Cq. perturbans* compared with laboratory-reared *An. gambiae* s.l. (Giles) (Sikulu et al. 2014) and *Ae. aegypti* (Sikulu-Lord et al. 2016). Study data at wavelengths corresponding to our spectrometer's resolution were converted from reflectance to absorbance and preprocessed using SNV, after which quartiles were calculated and outliers summed by age and weighted average age groups. As proof of concept, we applied the results for laboratory-reared *Ae. aegypti*, to wild-caught *Cq. perturbans* in order to classify collections as young or old cohorts. The minimum and maximum weighted average ages of laboratory-reared *Ae. aegypti* were correlated with maximum and minimum outlier fractions from *Cq. perturbans* collections without mites, with maximum *Ae. aegypti* age correlated to minimum *Cq. perturbans* outlier fraction and vice versa. When graphed, the slope formula from the derived coordinates was used to calculate an outlier fraction representing a wild-caught *Cq. perturbans* cohort with a weighted average age of 7 days. The calculated outlier fraction was then applied as a "7-day boundary" to age grade wild-caught collections of *Cq. perturbans* as young ($\leq$7 days) versus old ($>$7 days) based on the outlier fraction of the collection. The age grading was then correlated visually with abundance data for wild-caught *Cq. perturbans* from Anderson et al. (2018).

RESULTS

Economical NIRS system

The spectrometer and chassis were readily available; Table 1 details the cost of all components. System build took 3 days with most time spent anchoring the collimating lenses within the chassis. This was achieved by applying adhesive to the edges of the lenses with exceptional care to avoid contamination of lens or chassis interior reflecting surfaces. An additional 2 months were required to develop a standard operating procedure for scanning from experimentation with aspirin and correlation of in-house results to published spectra. Scanning software is available free of cost from the Texas Instruments website (https://www.ti.com/tool/DLPNIRNANOEVM) and functional on an HP Envy

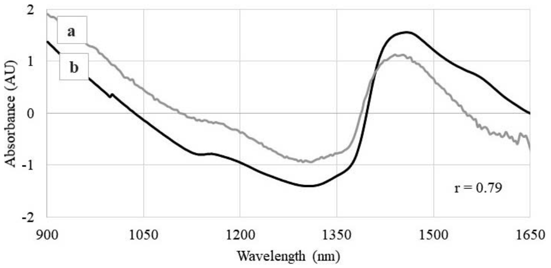

Fig. 4. Comparison of spectral averages of laboratory-reared day-old *Aedes aegypti*, showing strong correlation of our results with previously published data. (a) This study (*n* = 6). (b) Sikulu-Lord et al. (2016), generated using a LabSpec 5000 NIR spectrometer (*n* = 41).

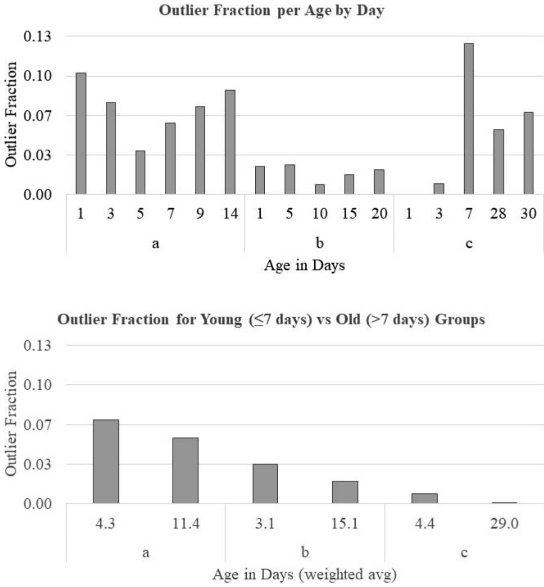

Fig. 5. Outlier fraction for female laboratory-reared mosquitoes by age in days and weighted average age in days. (a) Sikulu et al. (2014): *Anopheles gambiae* s.l., *n* = 295. (b) Sikulu-Lord et al. (2016): *Aedes aegypti*, *n* = 225. (c) This study: *Ae. aegypti*, *n* = 60.

360 laptop with an 8th-generation Intel® Core™ I5 processor (Hewlett-Packard Company, Palo Alto, CA).

Specimen preparation, scanning details, and data storage

We found that with practice, a batch of 20 mosquitoes could be prepared and scanned twice (40× scans) within 60 min. This included conducting background and aspirin scanning to verify system performance. An additional 30 min was needed for preparation when specimens were brittle, and wings and legs had to be removed in order to position the mosquito laterally for scanning. Individual files generated by the spectrometer in .csv format were migrated to Microsoft Access Version 2108 (Microsoft Corporation, Redmond, WA), resulting in a final file of 134.7 MB in size. All data querying and analysis were performed in Microsoft Access.

System calibration, modeling results, and outlier fraction analysis for Ae. aegypti

The spectra for laboratory-reared female *Ae. aegypti* generated by our system were very similar to those presented in Sikulu-Lord et al. (2016), and comparison of spectral averages as arrays for day-old mosquitoes (the only matching age between studies) showed a strong correlation to data from the prior study that incorporated a more sophisticated spectrometer, demonstrating a good calibration between systems (Fig. 4). Outlier fractions for age by day showed no trend (Fig. 5, top); however, when grouped by weighted average age into young versus old cohorts, the young cohorts showed a higher outlier fraction (Table 2 and Fig. 5, bottom). The PLS-1 modeling and prediction results on test sets of laboratory-reared *Ae. aegypti* showed that there were sufficient data for accurate prediction by weighted average age of young (≤7 days) versus old (>7 days) cohorts (Table 2 and Fig. 6). Comparisons of

Table 2. Laboratory-reared *Aedes aegypti*, simplified outlier analysis and modeling results.

		Simplified outlier analysis			Partial least squares (PLS-1) modeling: Age in days (weighted average)	
Mosquito age	*n*	TSDP[1]	Spectral outliers[2]	Outlier fraction[3]	Actual	Predicted (mean)
Sikulu-Lord et al. (2016)						
≤7 days	86	19,608	631	0.0322	3.1	5.1
>7 days	139	31,692	575	0.0181	15.1	14.5
This study						
≤7 days	38	8,664	69	0.0080[4]	4.4	7.1
>7 days	22	5,016	2	0.0004[4]	29.0	24.4

[1] Total spectral data points (TSDP) = *n* multiplied by spectrometer digital resolution of 228.
[2] Spectral outliers = points falling above or below TSDP quartiles.
[3] Outlier fraction = spectral outliers/TSDP.
[4] Reduction in outlier fraction as compared with Sikulu-Lord et al. (2016) may be caused by differences in equipment and instrumentation used, scanning technique, and total number of mosquitoes scanned per study.

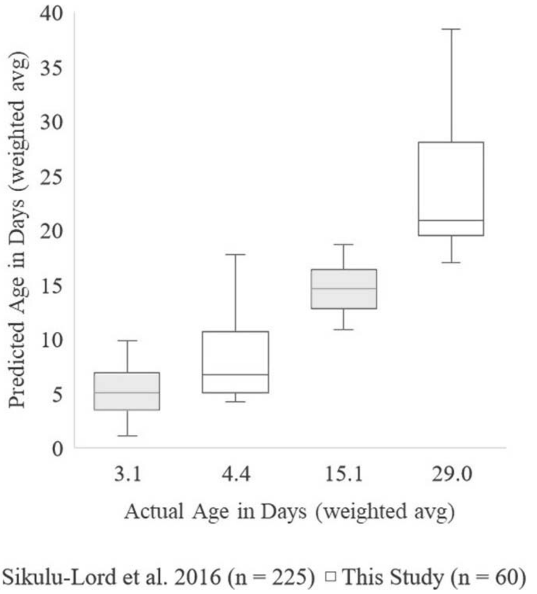

Fig. 6. Partial least squares (PLS-1) modeling prediction results for female laboratory-reared *Aedes aegypti*, young (≤7 days) versus old (>7 days) cohorts.

weighted average actual age versus outlier fraction ($r = -0.68$) and weighted average predicted age versus outlier fraction ($r = -0.71$) indicate that increased variation in spectra that leads to more outliers is an index of younger mosquitoes.

Modeling, outlier analysis, and age grading of Cq. perturbans

We found that modeling of *Cq. perturbans* could accurately predict cohorts by collection date with 85% accuracy on average, but also predicted different batches for the same date with 84% accuracy, and even differences in the same batch scanned twice consecutively with 98% accuracy. Predictive modeling results were similar for an uncoated aspirin pill scanned using the same procedure as for the mosquitoes. Subsequent analysis of SNV preprocessed spectra from the pill showed small shifts in absorption intensity between different scans, either as an increase (hyperchromic shift) or decrease (hypochromic shift) depending upon wavelength. Though the average difference in intensity between spectra was less than 1×10^{-15} AU, it is possible that PLS-1 modeling was sensitive enough to differentiate shifts by wavelength, hindering its use in this fashion for our setup.

For wild-caught *Cq. perturbans*, outliers typically occurred over the entire spectral region, as illustrated by the example box-whisker plots with a high and low number of outliers shown in Fig. 7. Collection abundance, scanning statistics, and outlier fraction details are shown in Table 3. Seasonal abundance (collection size) was lower with emergence occurring later for 2021 collections versus 2022 trap site D for the time periods trapped. Outlier fractions ranged from a high of 0.0352 at trap site B on August 10, 2021, to a low of 0.0035 for trap site D for the combined dates of August 23, 2022, and August 29, 2022. When all spectra were grouped into collections of mites versus no mites for 2021, the outlier fraction was slightly higher for mosquitoes infested with mites. However, no trends in outlier fractions were seen when 2022 mite and no-mite collections from several sites and dates were scanned individually (Fig. 8).

The average spectra of day-old laboratory-reared *Ae. aegypti* from our study and that of a collection of wild-caught *Cq. perturbans* with a high outlier fraction using our scanning setup was similar ($r = 0.96$) (Fig. 9), suggesting that age-related spectral variation may trend similarly across divergent mosquito taxa. Weighted average ages for *Ae. aegypti* from the combined data of Sikulu-Lord et al. (2016) and our study were calculated to be 3.5 and 17.0 days for young and old cohorts, respectively. These ages were matched to the maximum and minimum outlier fractions for collections of *Cq. perturbans* without mites from 2021 trap sites A and B and 2022 trap site D, and an outlier fraction of 0.027 for a weighted average age of 7 days was calculated from the slope of the coordinates (Fig. 10). This fraction was used as a 7-day boundary to classify collections of *Cq. perturbans* as either young or old. Figure 11 illustrates abundance versus cohorts classified as young or old for 2021 collections (Fig. 11a, 11b) and 2022 trap site D collections (Fig. 11c, 11d).

DISCUSSION

Cattail mosquitoes are one of the most widely distributed and prevalent human-feeding mosquitoes in North America and are thought to be major enzootic and zoonotic vectors. Cache Valley, eastern equine encephalitis, Flanders, Highlands J, Jamestown Canyon, Trivittatus, and West Nile viruses have all been isolated from *Cq. perturbans* (Andreadis et al. 2005). The seasonal abundance of the cattail mosquito in New England shows distinct pulses possibly indicating delays or staggering of seasonal emergence (Anderson et al. 2018), but population age distribution during the season has only been partially studied (Nasci et al. 1996, Ravenhurst 2013).

During eastern equine encephalitis outbreaks, the Massachusetts Department of Public Health conducts aerial spraying throughout the state of Massachusetts (Commonwealth of Massachusetts, Bureau of Infectious Disease and Laboratory Sciences, Department of Public Health 2022). Evaluation of such interventions is very difficult, given limitations on prespray sampling due to the dynamic nature of scheduling the spray event. As noted by other studies of adulticiding (Reisen et al. 1985, Reisen 2010), efficacy determinations may be confounded by the emergence of new

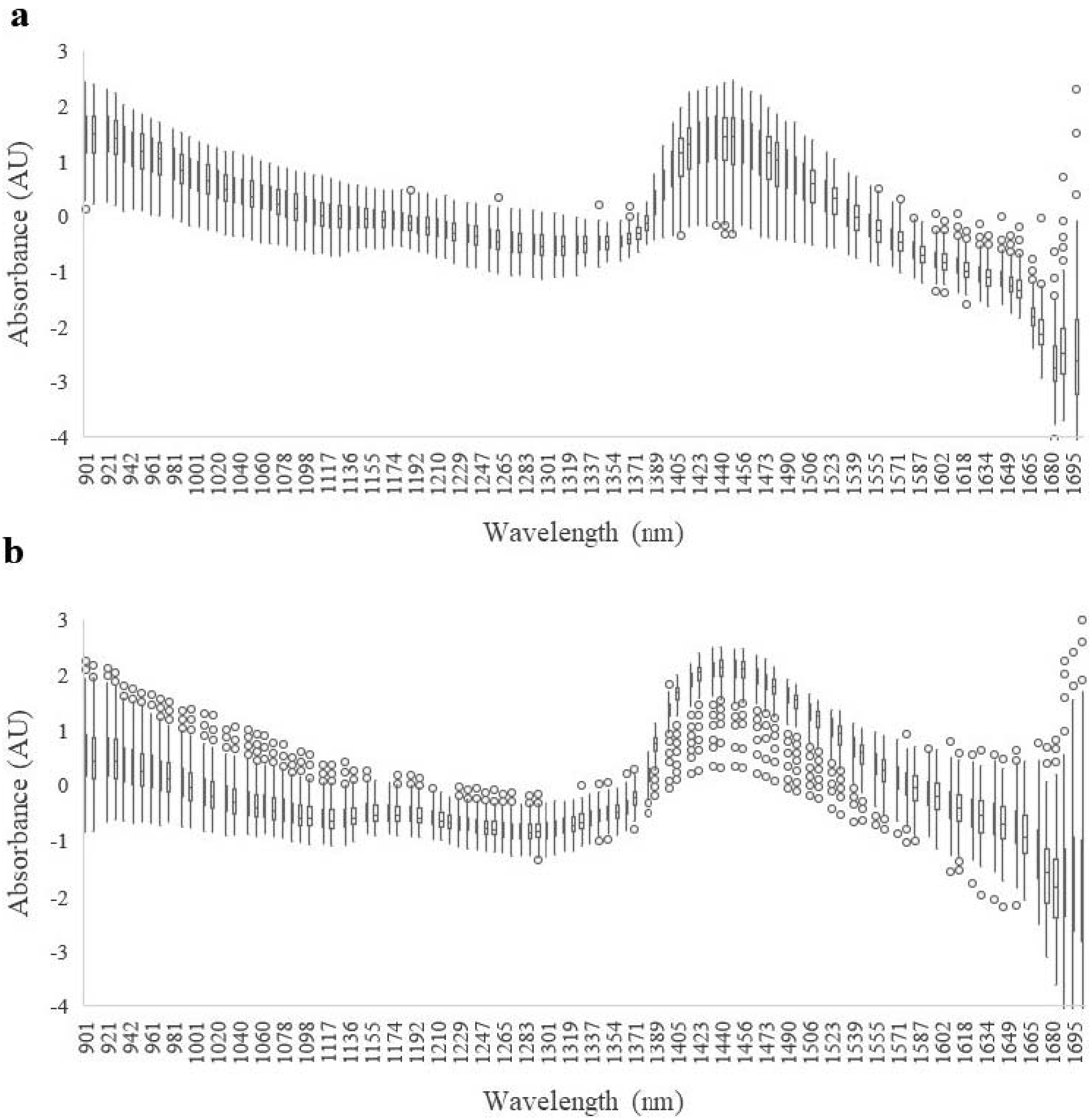

Fig. 7. Example wild-caught female *Coquillettidia perturbans* spectra box-whisker plots showing the location of outliers. (a) Low outlier fraction indicating an older cohort of mosquitoes: trap site A, July 20, 2021 ($n = 120$). (b) High outlier fraction indicating a younger cohort of mosquitoes: trap site B, August 3, 2021 ($n = 140$).

mosquitoes, and thus a failure to demonstrate a reduction in abundance indices does not necessarily imply failure of the intervention. However, such suggestions cannot be easily documented without age grading. The importance of providing an estimate of efficacy is that it may promote public support for an emergency public health measure that is highly controversial with environmental activists (Commonwealth of Massachusetts, Executive Office of Energy and Environmental Affairs, Mosquito Control for the Twenty-First Century Task Force 2021; Telford, unpublished data).

Coquillettidia perturbans is known as a univoltine species, with a single emergence each season (Crans 2004). As mosquitoes begin to emerge, abundance at the trap site peaks and the fraction of spectral outliers is large due to the influx of younger mosquitoes. As mosquitoes age and die off, abundance at the trap site and fraction of outliers decrease accordingly. For 2021, outlier trends from our data visually coincide with late-seasonal abundance for female wild-caught cattail mosquitoes (Fig. 12); however, the significant to critical drought experienced by Massachusetts in July and August of 2022 (Commonwealth of Massachusetts, Executive

Table 3. Collection results, scanning details, and outlier fraction estimates for wild-caught *Coquillettidia perturbans*. All trapping conducted via Centers for Disease Control and Prevention (CDC) miniature light trap with CO_2 as an attractant.

Trap site[1]	Collection date	Abundance[2]	Scanned	Scan count[3]	TSDP[4]	Outliers[5]	Outlier fraction[6]
2021: Without mites							
A	Jul 20, 2021	344	120	240	54,720	399	0.007
B	Jul 27, 2021	1,046	140	280	63,840	769	0.012
B	Aug 3, 2021	425	140	280	63,840	2,018	0.032
B	Aug 10, 2021	1,555	140	280	63,840	2,244	0.035
B	Aug 24, 2021	544	160	320	72,960	1,900	0.026
B	Aug 31, 2021	441	160	320	72,960	2,255	0.031
B	Sep 7–28, 2021[7]	99	99	198	45,144	319	0.007
	All collections	4,454	959	1,918	437,304	8,652	0.020
2021: With mites							
	All collections	112	112	224	51,072	1,324	0.026
2022: Without mites							
B	Jun 21, 2022	7,276	160	320	72,960	1,657	0.023
C	Jun 28, 2022	386	100	200	45,600	589	0.013
D	Jun 29, 2022	2,528	80	160	36,480	405	0.011
C	Jul 6, 2022	372	80	160	36,480	1,248	0.034
D	Jul 6, 2022	2,110	60	120	27,360	839	0.031
E	Jul 7, 2022	1,658	40	80	18,240	155	0.008
D	Jul 12, 2022	4,960	120	240	54,720	1,550	0.028
D	Jul 22, 2022	3,071	61	122	27,816	142	0.005
A	Jul 26, 2022	602	40	80	18,240	267	0.015
D	Jul 26, 2022	3,150	80	160	36,480	527	0.014
D	Aug 2, 2022	651	80	160	36,480	875	0.024
D	Aug 9, 2022	708	60	120	27,360	533	0.019
D	Aug 16, 2022	79	40	80	18,240	424	0.023
D	Aug 23–29, 2022[8]	18	18	36	8,208	29	0.004
2022: With mites							
B	Jun 21, 2022	413	100	200	45,600	649	0.014
C	Jun 28, 2022	41	40	80	18,240	232	0.013
C	Jul 6, 2022	44	41	82	18,696	260	0.014
E	Jul 7, 2022	112	40	80	18,240	35	0.002
D	Jul 12, 2022	301	41	82	18,696	86	0.005
D	Jul 22, 2022	126	46	92	20,976	229	0.011
A	Jul 26, 2022	55	40	80	18,240	267	0.015
D	Jul 26, 2022	124	44	88	20,064	86	0.004
D	Aug 2, 2022	35	30	60	13,680	105	0.008

[1] See Fig. 3 for trap site locations.
[2] Abundance = collection size, collected via CDC miniature light trap with CO_2 as an attractant.
[3] Each specimen scanned 2×.
[4] Total spectral data points (TSDP) = scan count multiplied by spectrometer digital resolution.
[5] Outliers = points falling above or below TSDP quartiles.
[6] Outlier fraction = spectral outliers/TSDP.
[7] September 7–28, 2021, abundance: Sep 7 = 54, Sep 14 = 8, Sep 21 = 20, Sep 28 = 17.
[8] August 23–29, 2022, abundance: Aug 23 = 12, Aug 29 = 6.

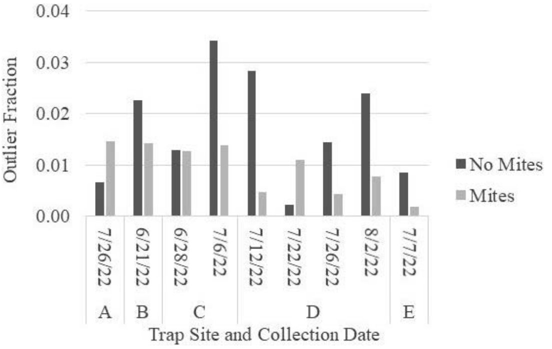

Fig. 8. Outlier fractions: *Coquillettidia perturbans* with mites and no mites for 2022 collections. Collection and scanning details are provided in Table 3; trap site locations are mapped in Fig. 3.

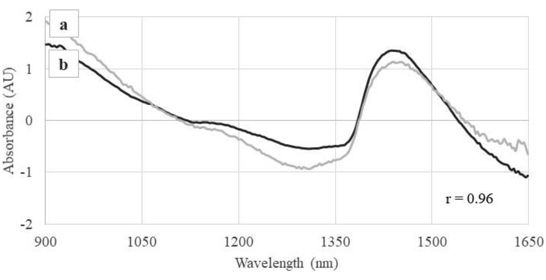

Fig. 9. Spectral averages illustrating the strong correlation between laboratory-reared and wild-caught mosquitoes. (a) This study, Tufts laboratory-reared day-old *Aedes aegypti* ($n = 6$). (b) Wild-caught *Coquillettidia perturbans*, trap site A, collected with a miniature Centers for Disease Control and Prevention (CDC) light trap with CO_2 as an attractant, July 20, 2021 ($n = 120$).

Fig. 10. Minimum and maximum weighted average age of laboratory-reared *Aedes aegypti* (Sikulu-Lord et al. 2016 and this study) assigned to maximum and minimum outlier fractions of wild-caught *Coquillettidia perturbans* without mites (Table 3), with a calculated fraction of 0.027 at 7 days set as a boundary to classify wild-caught collections of *Cq. perturbans* as either young (≤7 days) or old (>7 days).

Office of Energy and Environmental Affairs, Drought Management Task Force 2022) most likely impacted the timing and number of emergences, potentially causing the sharp drop in abundance in August 2022 at trap site D (Fig. 11c). The shift in July–August emergence timing between trap sites from later in 2021 to earlier in 2022 corresponds to the shift in cohorts classified as young versus old (Fig. 11b, 11d), suggesting that outlier analysis performed consistently between the 2 different sites and seasons, and that differences in cattail mosquito larval habitat and diet did not have a pronounced impact on results. Other studies have suggested the possibility that there are pulses of delayed emergence from the single brood, likely due to local variation in water temperature or other factors that impact larval instar development (Bosak 1996, 2002; Crans 2004). Such emergence dynamics may influence arboviral transmission and human risk and require further study.

Simplified outlier analysis showed no trend in mosquitoes with mites versus those without for 2022 collections (Fig. 8); however, our investigation is not definitive since mite species and condition at the time of collection were not verified, and the reliability of age grading using mites is dependent upon mite species, condition at the time of collection, and the fraction of parasitized mosquitoes in the population (Corbet 1963, Silver 2008). The technique may also be undependable when mite incidence is less than 5% (Corbet 1970, Morris and DeFoliart 1970), and the overall presence of mites for all 2022 collections was only 4.5% (Table 3).

Age grading of wild cohorts using spectral data from laboratory-reared specimens has been found to be acceptable if spectra from laboratory-reared and wild mosquitoes are similar for age and species (Milali et al. 2018), and we have shown strong correlation between laboratory-reared and wild-caught mosquitoes of different species in spectra

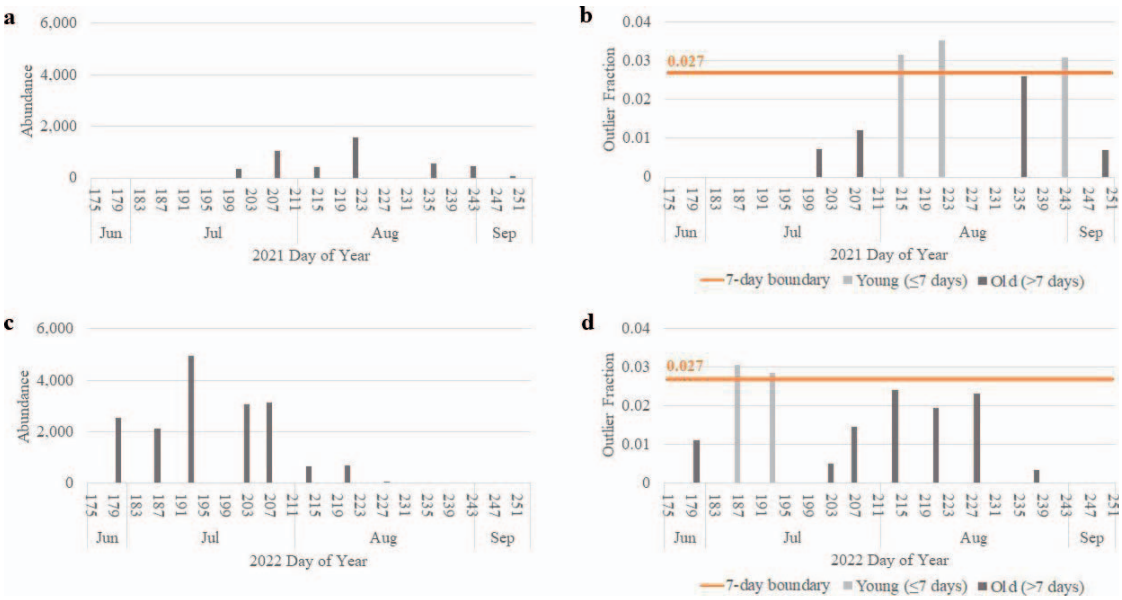

Fig. 11. Wild-caught *Coquillettidia perturbans* without mites, 2021 trap sites A and B, and 2022 trap site D; abundance (collection size) versus outlier fraction. Collection and scanning details are provided in Table 3; trap site locations are mapped in Fig. 3. The above graphs show: (a) trap sites A and B, 2021 abundance; (b) trap sites A and B, 2021 classification into young or old cohorts based on the calculated 7-day boundary outlier fraction (0.027) from Fig. 9; (c) trap site D, 2022 abundance; and (d) trap site D, 2022 classification into young or old cohorts based on the calculated 7-day boundary outlier fraction (0.027) from Fig. 9.

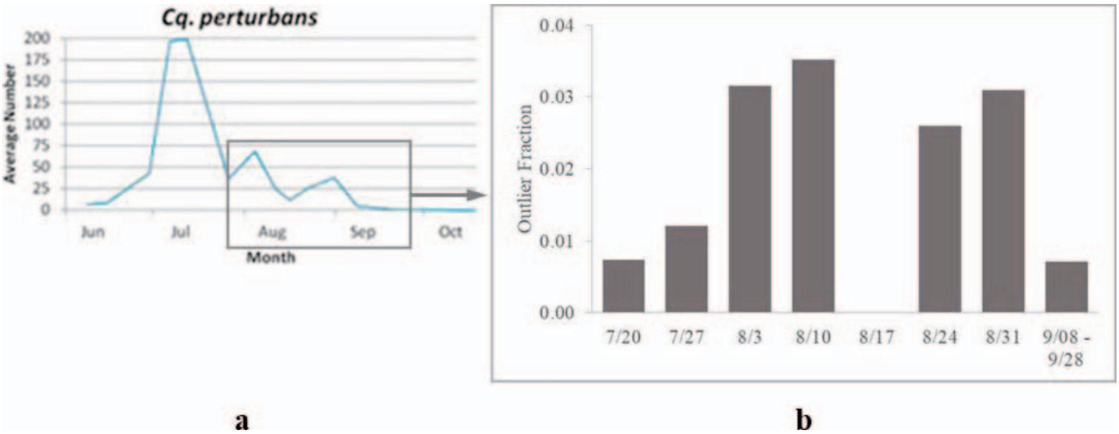

Fig. 12. Wild-caught *Coquillettidia perturbans* seasonal distribution, abundance versus outlier fraction: (a) abundance (Anderson et al. 2018, fig. 3) and (b) trap sites A and B 2021 outlier fraction, this study.

generated by our system (Fig. 9). Though the negative trend in outlier fraction for young versus old laboratory-reared cohorts is the same in our study as in prior studies, our values are smaller than those of the prior studies (Table 2 and Fig. 5, bottom). The smaller outlier fractions in our study may be due to differences in scanning technique and systems, or the fewer number of mosquitoes scanned. These differences indicate that ideally laboratory-reared and wild-caught species and scanning systems should be the same for future investigations of age grading of wild cohorts using the simplified outlier method, and that our study is a proof of concept only. However, age grading based on spectra from a different species of laboratory-reared mosquito may be the only viable option for *Cq. perturbans*, since cattail mosquitoes have not been stably colonized in the laboratory due to the unique biology of their larvae, which obligately attach to the roots of emergent aquatic plants (Crans 2004). Regardless, further work is needed to refine and validate the simplified outlier method through development of benchmark outlier fractions by age for different mosquito species based on laboratory-reared specimens of known age. The basis of differences in outlier frequency between young and old mosquitoes might thereby be determined, e.g., whether it is produced by cuticle damage (younger mosquitoes show greater variation in the amount of damage sustained to their cuticle due to their shorter life spans), changes in hydrocarbons over time (cuticles become more uniform as mosquitoes age), or some other means. All specimens scanned for this study were "fresh frozen," and the impact of differing lengths of frozen storage should also be investigated.

Additional study is needed to determine whether the method has the potential to identify weighted average age in days with greater granularity for wild-caught cohorts. The full range of outlier fractions might be obtained from mosquito collections made throughout an entire season or by allowing captures to age within outdoor cages. Moreover, the method could provide training and correlation data for deep transfer learning modeling of the type developed by Siria et al. (2022) for predicting control efficacy.

We conclude that this low-cost and rapid technique shows promise for studying the age of wild mosquito populations and could easily be integrated into the evaluation of mosquito control efficacy. Spectra generated from this economical method compare favorably to previous studies utilizing laboratory-grade spectrometers and reflectance standards. Our results are consistent with analysis of literature data from prior NIRS investigations of laboratory-reared mosquitoes of known age. An analysis of field-collected *Cq. perturbans*, using the simple spectral analysis outlier method for assigning mosquitoes to young or old cohorts, suggests that there may be complex emergence dynamics within a transmission season even with a univoltine vector: although there is likely only a single emergence each season, local conditions may delay full development and cattail mosquitoes may emerge into August.

ACKNOWLEDGMENTS

The authors thank Timothy D. Deschamps, Central Massachusetts Mosquito Control Project. CLS would like to thank Christopher Lee of Boston College for his help with cabinetry construction. The following reagent was provided by the NIH/NIAID Filariasis Research Reagent Resource Center for distribution through BEI Resources, NIAID, NIH: *Aedes aegypti*, Strain Black Eye Liverpool, Eggs, NR-48921. CLS and SRT are supported, in part, by grants from the NIH (RO1 AI 137424, AI 130105), the Evelyn Lilly Lutz Foundation, the Rainwater Foundation, and a gift from Catherine C. Lastavica.

REFERENCES CITED

Anderson JF, Armstrong PM, Misencik MJ, Bransfield AB, Andreadis TG, Molaei G. 2018. Seasonal distribution, blood-feeding habits, and viruses of mosquitoes in an open-faced quarry in Connecticut, 2010 and 2011. *J Am Mosq Control Assoc* 34:1–10.

Andreadis TG, Thomas MC, Shepard JJ. 2005. Identification guide to the mosquitoes of Connecticut. *Bull Conn Agric Exp Stn* 966:1–173.

Bosak PJ. 1996. *Population dynamics of* Coquillettidia perturbans *and its relevance to Eastern Equine Encephalitis virus in New Jersey* [Internet]. In: *42nd Annual meeting of the Northeastern Mosquito Control Association*. 1996 December 9–11; Mystic, CT. Hamden, CT: Northeastern Mosquito Control Association, Inc. [accessed April 12, 2022]. 5 p. Available from: http://www.nmca.org/paper21a.htm.

Bosak PJ. 2002. *Behavioral and morphological aspects of the cattail mosquito,* Coquillettidia perturbans *(Walker) in relation to Eastern Equine Encephalomyelitis virus in New Jersey* [Ph.D. dissertation]. The State University of New Jersey, Rutgers, NJ. 148 p.

Commonwealth of Massachusetts, Bureau of Infectious Disease and Laboratory Sciences, Department of Public Health. 2022. *Mosquito control and spraying, fact sheet about aerial spraying of mosquitoes for EEE* [Internet]. Jamaica Plain, MA: Commonwealth of Massachusetts [accessed August 8, 2022]. Available from: https://www.mass.gov/service-details/mosquito-control-and-spraying.

Commonwealth of Massachusetts, Department of Public Health, State Laboratory Institute. 2022. *MDPH Arbovirus Surveillance Database* [Internet]. Jamaica Plain, MA: Commonwealth of Massachusetts [accessed January 1, 2022]. Available from: https://wnv.dph.state.ma.us/WNV/wnvLogin.aspx.

Commonwealth of Massachusetts, Executive Office of Energy and Environmental Affairs, Drought Management Task Force. 2022. *Drought status* [Internet]. Boston, MA: Commonwealth of Massachusetts [accessed September 20, 2022]. Available from: https://www.mass.gov/info-details/drought-status#past-droughts-and-declaration-.

Commonwealth of Massachusetts, Executive Office of Energy and Environmental Affairs, Mosquito Control for the Twenty-First Century Task Force. 2021. *Study prepared for the Mosquito Control for the Twenty-First Century Task Force, Appendix B ERG Report for the Mosquito Control for the Twenty-First Century Task Force* [Internet]. August 2021. Boston, MA: Commonwealth of Massachusetts [accessed September 25, 2022]. Available from: https://www.mass.gov/doc/appendix-b-erg-report-for-the-mosquito-control-for-the-twenty-first-century-task-force/download.

Corbet PS. 1963. Reliability of parasitic water-mites (Hydracarina) as indicators of physiological age in mosquitoes (Diptera: Culicidae). *Entomol Exp Appl* 6:215–233.

Corbet PS. 1970. The use of parasitic water-mites for age-grading female mosquitoes. *Mosq News* 30:436–438.

Crans WJ. 2004. A classification system for mosquito life cycles: life cycle types for mosquitoes of the northeastern United States. *J Vector Ecol* 29:1–10.

Dowell FE, Noutcha AEM, Michel K. 2011. Short Report: The effect of preservation methods on predicting mosquito age by near infrared spectroscopy. *Am J Trop Med Hyg* 85:1093–1096.

Garrett-Jones C, Grab B. 1964. The assessment of insecticidal impact on the malaria mosquito's vectorial capacity, from data on the proportion of parous females. *Bull WHO* 31:71–86.

Janecek M. 2012. Reflectivity spectra for commonly used reflectors. *IEEE Trans Nucl Sci* 59:490–497.

Johnson JB, Naiker M. 2020. Seeing red: a review of the use of near-infrared spectroscopy (NIRS) in entomology. *Appl Spectrosc Rev* 55:810–839.

Joy T, Chen M, Arnbrister J, Williamson D, Li S, Nair S, Brophy M, Garcia VM, Walker K, Ernst K, Gouge DH, Carrière Y, Riehle MA. 2022. Assessing near-infrared spectroscopy (NIRS) for evaluation of *Aedes aegypti* population age structure. *Insects* 13:360.

Krajacich BJ, Meyers JI, Alout H, Dabiré RK, Dowell FE, Foy BD. 2017. Analysis of near infrared spectra for age-grading of wild populations of *Anopheles gambiae*. *Parasit Vectors* 10:552.

Lambert B, Sikulu-Lord MT, Mayagaya VS, Devine G, Dowell F, Churcher TS. 2018. Monitoring the age of mosquito populations using near-infrared spectroscopy. *Sci Rep* 8:5274.

Liebman K, Swamidoss I, Vizcaino L, Lenhart A, Dowell F, Wirtz R. 2015. The influence of diet on the use of near-infrared spectroscopy to determine the age of female *Aedes aegypti* mosquitoes. *Am J Trop Med Hyg* 92:1070–1075.

Martinson VG, Strand MR. 2021. Diet-microbiota interactions alter mosquito development. *Front Microbiol* 12:650743.

Milali MP, Kiware SS, Govella NJ, Okumu F, Bansal N, Bozdag S, Charlwood JD, Maia MF, Ogoma SB, Dowell FE, Corliss GF, Sikulu-Lord MT, Povinelli RJ. 2020. An autoencoder and artificial neural network-based method to estimate parity status of wild mosquitoes from near-infrared spectra. *PLoS ONE* 15:e0234557.

Milali MP, Sikulu-Lord MT, Kiware SS, Dowell FE, Povinelli RJ, Corliss GF. 2018. Do NIR spectra collected from laboratory-reared mosquitoes differ from those collected from wild mosquitoes? *PLoS ONE* 13:e098245.

Morris CD, DeFoliart GR. 1970. The physiological age of Wisconsin *Aedes* mosquitoes parasitized by water-mites. *J Med Entomol* 7:628.

Nasci RS, Berry RL, Restifo RA, Moore CG. 1996. Population size, parity structure, and wing length of *Coquillettidia perturbans* in an Ohio focus of Eastern Equine Encephalitis. *J Am Mosq Control Assoc* 12:64–68.

Ong OTW, Kho EA, Esperança PM, Freebairn C, Dowell FE, Devine GJ, Churcher TS. 2020. Ability of near-infrared spectroscopy to predict the age of mosquitoes reared under different conditions. *Parasit Vectors* 3:160.

Ravenhurst J. 2013. *Ovary dissections for parity determination of field-collected* Coquillettidia perturbans *mosquitoes in central Massachusetts* [Internet]. Northborough, MA: Central Massachusetts Mosquito Control Project [accessed December 13, 2021]. 8 p. Available from: https://www.cmmcp.org/sites/g/files/vyhlif2966/f/uploads/2013_ovary_dissections_for_parity_determination.pdf.

Reisen WK. 2010. Using "Mulla's Formula" to estimate percent control. In: Atkinson PW, ed. *Vector biology, ecology, and control*. New York, NY: Springer SBM. p 127–138.

Reisen WK, Milby MM, Reeves WC, Eberle MW, Meyer RP, Schaefer CH, Parman RB, Clement HL. 1985. Aerial adulticiding for the suppression of *Culex tarsalis* in Kern County, California, using low volume propoxur: 2.

Impact on natural populations in foothill and valley habitats. *J Am Mosq Control Assoc* 1:154–163.

Sikulu M, Killeen GF, Hugo LE, Ryan PA, Dowell KM, Wirtz RA, Moore SJ, Dowell FE. 2010. Near-infrared spectroscopy as a complementary age grading and species identification tool for African malaria vectors. *Parasit Vectors* 3:49.

Sikulu MT, Majambere S, Khatib BO, Ali AS, Hugo LE, Dowell FE. 2014. Using a near-infrared spectrometer to estimate the age of *Anopheles* mosquitoes exposed to pyrethroids. *PLoS ONE* 9:e90657. Study data available as supplementary material from: https://www.nature.com/articles/s41598-018-22712-z#Sec7. [accessed February 2, 2021].

Sikulu-Lord MT, Milali MP, Henry M, Wirtz RA, Hugo RE, Dowell FE, Devine GJ. 2016. Near-infrared spectroscopy, a rapid method for predicting the age of male and female wild-type *Wolbachia* infected *Aedes aegypti*. *PLoS Negl Trop Dis* 10:e0005040. Study data available as supplementary material from: https://www.nature.com/articles/s41598-018-22712-z#Sec7. [accessed February 2, 2021].

Silver JB. 2008. *Mosquito ecology: field sampling methods*. 3rd edition. Dordrecht, Netherlands: Springer.

Siria DJ, Sanou R, Mitton J, Mwanga EP, Niang A, Sare I, Johnson PCD, Foster GM, Belem AMG, Wynne K, Murray-Smith R, Ferguson HM, González-Jiménez M, Babayan SA, Diabaté A, Okumu FO, Baldini F. 2022. Rapid age-grading and species identification of natural mosquitoes for malaria surveillance. *Nat Commun* 13:1501.

Texas Instruments Inc. 2015. *TIDA-00554 Test Results (DLP ® Ultra - Mobile Near - Infrared Spectrometer)* [Internet]. Dallas, TX: Texas Instruments Inc. [accessed May 12, 2020]. Available from: https://www.ti.com/lit/ug/tidua82/tidua82.pdf?ts=1639506522637&ref_url=https%253A%252F%252Fwww.google.com%252F.

Williams P. 2013. The bounty of precision. *NIR News* 24:4.